Hindawi Publishing Corporation
Advances in Materials Science and Engineering
Volume 2013, Article ID 578434, 7 pages
http://dx.doi.org/10.1155/2013/578434

Research Article

$SmBa_2NbO_6$ Nanopowders, an Effective Percolation Network Medium for YBCO Superconductors

S. Vidya,[1] K. C. Mathai,[1] P. P. Rejith,[1] Sam Solomon,[2] and J. K. Thomas[1]

[1] *Electronic Materials Research Laboratory, Department of Physics, Mar Ivanios College, Thiruvananthapuram, Kerala 695015, India*
[2] *Dielectric Materials Research Laboratory, Department of Physics, St. John's College, Kollam District, Anchal, Kerala 691306, India*

Correspondence should be addressed to J. K. Thomas; jkthomasemrl@yahoo.com

Received 30 May 2013; Accepted 29 August 2013

Academic Editor: John W. Gillespie

The percolation behavior of superconductor-insulator composite, $YBa_2Cu_3O_{7-\delta}$, and nano $SmBa_2NbO_2$ synthesized by modified combustion technique was studied. Particle size of nano $SmBa_2NBO_6$ was determined using transmission electron microscopy. The chemical nonreactivity of nano $SmBa_2NbO_6$ with YBCO is evident from the X-Ray diffraction study which makes it a suitable nanoceramic substrate material for high temperature superconducting films. A systematic increase in the sintered density, approaching the optimum value of the insulating nanophase is clearly observed, as the vol.% of YBCO in the composite decreases. SEM micrograph showed uniform distribution of nanopowder among the large clusters of YBCO. The obtained percolation threshold is ~26 vol% of YBCO in the composite. All the composites below the threshold value showed $T_{C(0)} \sim 92$ K even though the room resistivity increases with increase in vol.% of nano $SmBa_2NbO_6$. The values of critical exponents obtained matches well with the theoretically expected ones for an ideal superconductor-insulator system.

1. Introduction

Superconductor-insulator composite can be regarded as the superconducting links embedded in a nonsuperconducting host material. Such composite are reported to possess novel properties, completely different from its pure superconductor state [1, 2]. A noticeable feature is the improvement of the critical current density, flux pinning, and broad range of current carrying capacity which makes these superconducting composites apt for superconducting fault current limiters (SFCL) [3–5]. The addition of nanoparticles which act as artificial pinning centers in the superconductor further enhances its transport properties.

The study of superconducting small aggregates, clusters, and particles is very important from both fundamental and technological stand point [6–8]. Due to the granular nature of these materials with short coherence length and large penetration depth, it is interesting to study the percolation and superconductivity of composites consisting of a superconductor embedded in an insulator medium [9, 10]. The percolation studies in metal-insulator composites are possible only on composite systems which are chemically nonreacting under the high processing temperature. In the case of percolation model of superconductor-insulator composite, the critical volume fraction of superconductor required to have a continuous network or to become an infinite cluster is called the percolation threshold value. The percolation studies conducted in high T_C superconductor shows almost zero resistance up to a particular insulator composition, known as percolation threshold above which the composite is a perfect insulator. This superconductor-insulator transition was explained in numerous ways based on different theoretical and experimental results. In the case of superconductor-insulator composites, there exists a long-range connectivity of superconducting grains within the insulating ceramic above the percolation threshold below which these weak links break up and superconductivity ceases. According to the scaling theory suggested by Fisher et al. [11, 12], if the superconductivity is ruined by phase fluctuations, then the superconducting phase can be considered to be a condensate of Cooper pairs with localized vortices and the insulating phase as a condensate of vortices with localized Cooper pairs.

At the time of transition, both vortices and Cooper pairs are mobile which results in a finite resistance, thereby destroying the superconductivity. In ultrathin films, this is assumed to occur at the absolute zero of temperature where the phase transitions are driven purely by quantum fluctuations rather than normal temperature phase transitions in which thermal fluctuations are critical [13, 14]. Finite temperature behavior in the vicinity of a quantum critical point was also studied [15, 16], in which the density of states and the Cooper pairing are suppressed on the insulating side due to an enhanced Coulomb interaction. The superconductor-insulator transition occurs as a consequence of fluctuations in the amplitude, rather than the phase of the order parameter. In other words, Cooper pairs break up into single electrons at the transition. Therefore, the superconducting gap would also vanish at the transition. Mitsen and Ivanenko [17] reported the presence of intermediate concentration region when the negative U-centers are formed during insulator to conductor state in HTS under doping. A study on superconductor-insulator transition in two dimensions was done by Marković et al. [18]. A numerical simulation was developed by Strelniker et al. to determine the critical resistance value, separating the superconducting and insulating branches [19]. The substrate applications and percolation studies of the superconductor-insulator composites were reported by Koshy et al., in which they used the conventional solid state processed ceramic powder [20–22].

Normally, a high T_C superconductor-insulator system is difficult to obtain without compromising the superconducting properties. High T_C superconductors require prolonged heating at the processing temperature (>900°C) and most of the system do react chemically with each other under such annealing condition thereby destroying the superconductivity. In the present paper, we report the synthesis of nano $SmBa_2NbO_6$ through a modified combustion route, the electrical transport studies and percolation behavior of $YBa_2Cu_3O_{7-\delta}$ nano $SmBa_2NbO_6$, superconductor-insulator composite system in detail.

2. Experimental

2.1. Combustion Technique. In a typical modified combustion synthesis, aqueous solution containing ions of Sm, Ba, and Nb is prepared by dissolving stoichiometric amount of high purity Sm_2O_3 in concentrated HNO_3, $Ba(NO_3)_2$ in double distilled water and $NbCl_5$ in hot oxalic acid. Citric acid was added as a complexing agent maintaining the citric acid to the cation ratio at unity. Amount of citric acid was calculated based on total valence of the oxidizing and the reducing agents for maximum release of energy during combustion. Appropriate amount of urea which acts as fuel was added to the precursor solution. Oxidant/fuel ratio of the system was adjusted by adding conc. nitric acid. The precursor solution is acidic in nature. The solution containing the precursor mixture was heated using a hot plate at ~250°C in a ventilated fume hood. The solution boils on heating and undergoes dehydration accompanied by foam. The foam get ignites by itself on persistent heating giving voluminous and fluffy product of combustion. The obtained powder is annealed at oxygen atmosphere at 1000°C for 30 minutes in order to eliminate trace amount of organic impurity that may remain in sample, and the obtained powder is characterized as single-phase nanocrystals of $SmBa_2NbO_6$.

2.2. Preparation of $YBa_2Cu_3O_{7-\delta}$-$SmBa_2NbO_6$ Composites. Pure $YBa_2Cu_3O_{7-\delta}$ (YBCO) was prepared from high purity Y_2O_3, $BaCO_3$, and CuO by solid state reaction. The powder was then calcined at 900°C for 52 h with two intermediate wet grindings. A 1:1 (v/v) mixture of finely powdered $SmBa_2NbO_6$ and YBCO was thoroughly mixed and pressed in the form of circular discs. The samples were sintered at 950°C for 24 h with a heating rate of 3°C/min and then cooled to 550°C in 8 h, kept for 24 h oxygenation. The compound $SmBa_2NbO_6$ (SBNO) was prepared by combustion technique was used for preparing the composites. The YBCO-SBNO composites have been prepared by mixing different volume percentages of YBCO and SBNO. The samples were pressed in the form of pellets and sintered at temperatures in the range of 950°C to 1350°C for 24 h in air depending upon the volume percentage of SBNO in the composite. It was observed that as the vol.% of SBNO in the composite increases the sintering temperature also increases. The samples were then cooled slowly to room temperature in air. For YBCO-SBNO composites containing upto 70 vol.% of SBNO the sintering temperature was <1020°C and for composites containing SBNO > 70 vol%, the sintering temperature had to be increased above 1020°C.

2.3. Characterization. Structure and Chemical stability of the nanopowder, pure YBCO and the composites were examined by powder X-ray diffraction (XRD) technique using a Bruker D-8 X-ray Diffractometer with Nickel filtered Cu K_α radiation. Particulate properties of the combustion product were examined using transmission electron microscopy (TEM, Model-Hitachi H-600 Japan) operating at 200 kV. The surface morphology of the sintered samples was examined using scanning electron microscopy (SEM) (Model-Hitachi S 2400 Japan). The Temperature-resistivity response of the YBCO-SBNO composite was measured by standard four probe technique using a nanovoltmeter (Keithley, model 2400), a current source (Keithley, model 2182A), and LS325 lakeshore temperature controller with PT111 sensor.

3. Results and Discussions

The powder morphology of the as-prepared $SmBa_2NbO_6$ (SBNO) obtained by the combustion synthesis is studied with transmission electron microscope (TEM) image and is given in Figure 1. TEM micrograph showed that the nanoparticles are of cuboidal shape and have particle size in the range 15–20 nm. The nanoparticles are little agglomerated with well defined particle morphology which points to the excellent nanonature of the sample. This nanopowder as such is used for further percolation characteristic studies.

The X-ray diffraction studies were carried out to identify different phases existing in YBCO-SBNO composite and to see the extent of reactions between the two compounds.

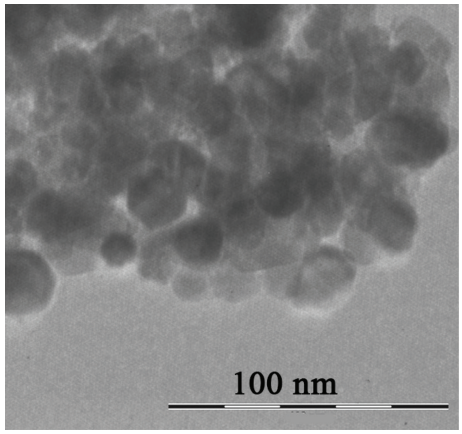

Figure 1: TEM image of as prepared nano $SmBa_2NbO_6$.

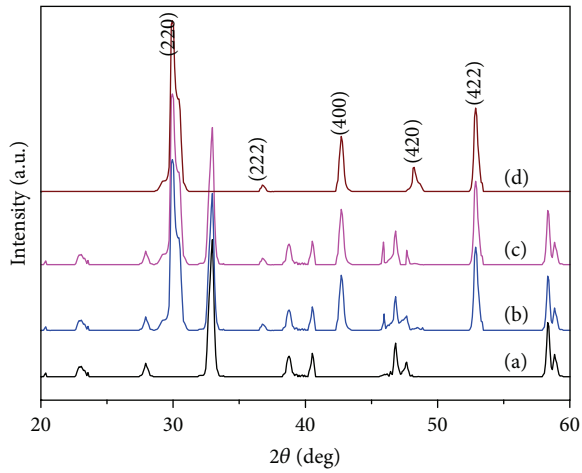

Figure 2: XRD patterns of (a) pure 100% YBCO, (b) 50% YBCO + 50% SBNO, (c) 70% YBCO + 30% SBNO, and (d) 100% SBNO.

The XRD patterns of YBCO-SBNO composites for 0 to 100 vol.% of SBNO in the system are given in Figure 2. In the XRD patterns of the composites upto 70 vol.% of SBNO, two distinct sets of peaks, one corresponding to YBCO having an orthorhombic structure and the other corresponding to SBNO, are clearly visible. There is no evidence of any additional peaks other than those of YBCO and SBNO in the XRD patterns indicating that, there is no detectable reaction between the two compounds even after severe heat treatment upto 1020°C.

In the case of almost all known ceramic insulators, the superconducting properties of YBCO and its orthorhombic structure is lost when it is processed along with the insulator above 950°C, but in the case of YBCO-SBNO, the structure and superconducting properties of YBCO are not affected even after a severe heat treatment above 1000°C for a prolonged period.

For YBCO-SBNO composites with SBNO greater than 70% the sintering temperature is greater than the peritectic temperature (1030°C) of YBCO above which the formation of insulating phase 211 is expected, but the XRD pattern does not shows any such inclusion of 211 phase.

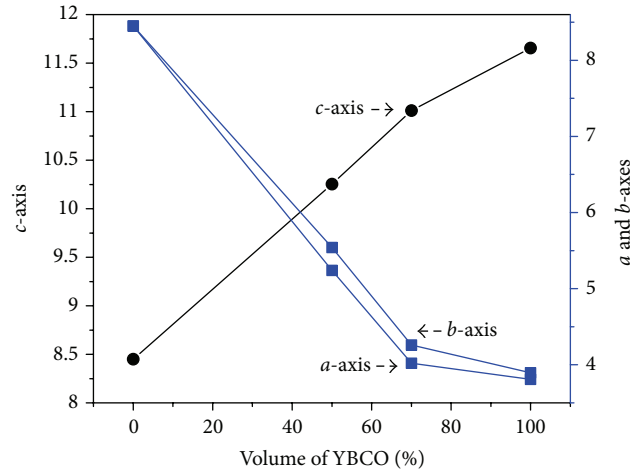

Figure 3: Variation of a, b and c-axes of YBCO with increasing SBNO addition.

Table 1: Sintering temperature and density of YBCO-SBNO composites.

Sample	Sintering temperature (°C)	Density (g/cc)
100 YBCO	920	5.32
80 YBCO + 20 SBNO	920	5.35
50 YBCO + 50 SBNO	950	5.44
30 YBCO + 70 SBNO	1100	5.68
100 SBNO	1350	6.25

The variation of a, b, and c-axis length of YBCO superconductor with the increasing content of SBNO in the composite is shown in Figure 3.

As the volume percentage of SBNO increases, the lattice parameters of YBCO decrease even though YBCO retains its orthorhombic structure.

3.1. Microstructure Analysis. Many properties of a macroscopic system are essentially determined by the connectivity of the system elements. The properties of a system which emerge at the onset of macroscopic connectivity within it are known as percolation properties. Thus, microstructure analysis has great relevance in understanding the intergrain connectivity. YBCO-SBNO composites are sintered in the temperature range 920°C to 1350°C.

The sintering temperature and densities achieved by each sample are listed in the Table 1.

The microstructure of the composites are analyzed by SEM images shown in Figure 4. The SEM images clearly shows the presence of white inclusions of SBNO uniformly distributed among the bulk YBCO samples. The nanograins of SBNO were grown as large interconnected platelets without any crack during sintering process which appears in white particles that are incorporated in between large YBCO clusters. However, there are different grain sizes and a random orientation of grain boundaries, whereby, it is expected the presence of different intergrain conductivities.

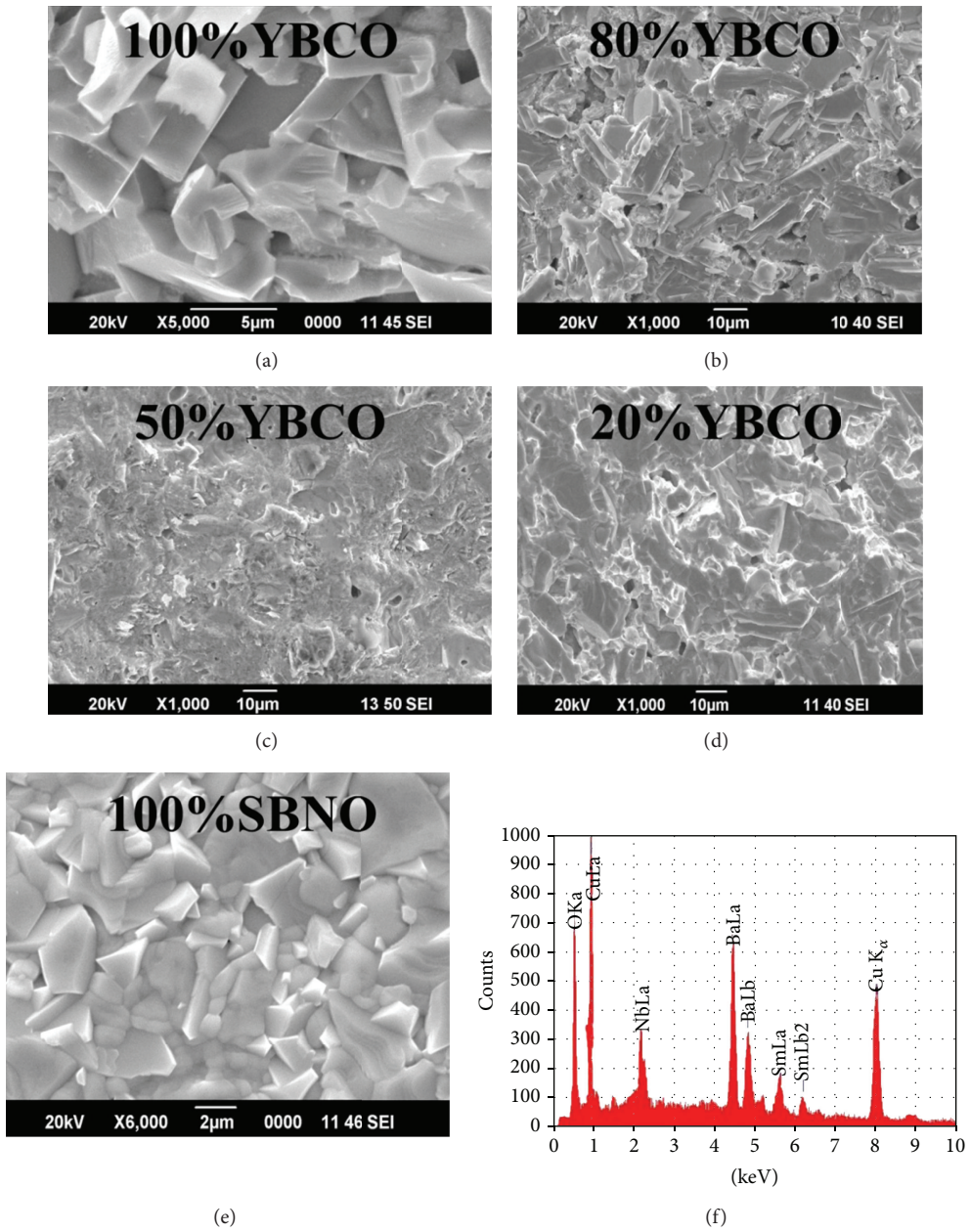

Figure 4: SEM images of different compositions of YBCO-SBNO composite and EDAX spectrum of a 1:1 mixture of YBCO and SBNO.

The EDAX spectrum of a 1:1 mixture of YBCO and SBNO is also shown in the Figure 4. It can be seen that apart from the stoichiometric ratio of components elements of the composite, no other impurity is present in the composite.

3.2. Temperature-Resistivity Measurements. The resistivity of the YBCO-SBNO composites with different volume percentages of SBNO were measured by four-probe method in the temperature range 300–77 K. The temperature dependence of normalized with different volume percentages of SBNO is shown in Figure 5.

Composites up to 70 vol.% of SBNO showed metallic behaviour and gave a zero resistivity superconducting transition temperature above 90 K. Even though there is superconducting transition for 80 vol% of SBNO in the composite, its resistivity does not become zero even up to 77 K. This can be due to the absence of the superconducting network throughout the matrix of the composite because of low volume percentage of YBCO in the composite. Samples with higher vol.% of SBNO say greater than 80% exhibited high value of resistance in the normal temperature, and a two-probe method was used to measure their resistivity.

The superconducting percolation threshold of YBCO-SBNO composites lies between 20 and 29 vol.% of YBCO in the composite. This means that, when the volume percentage of YBCO is 30 or above, there are interconnected networks of superconducting grains for the super current to pass through the composite material, but for lower volume percentage

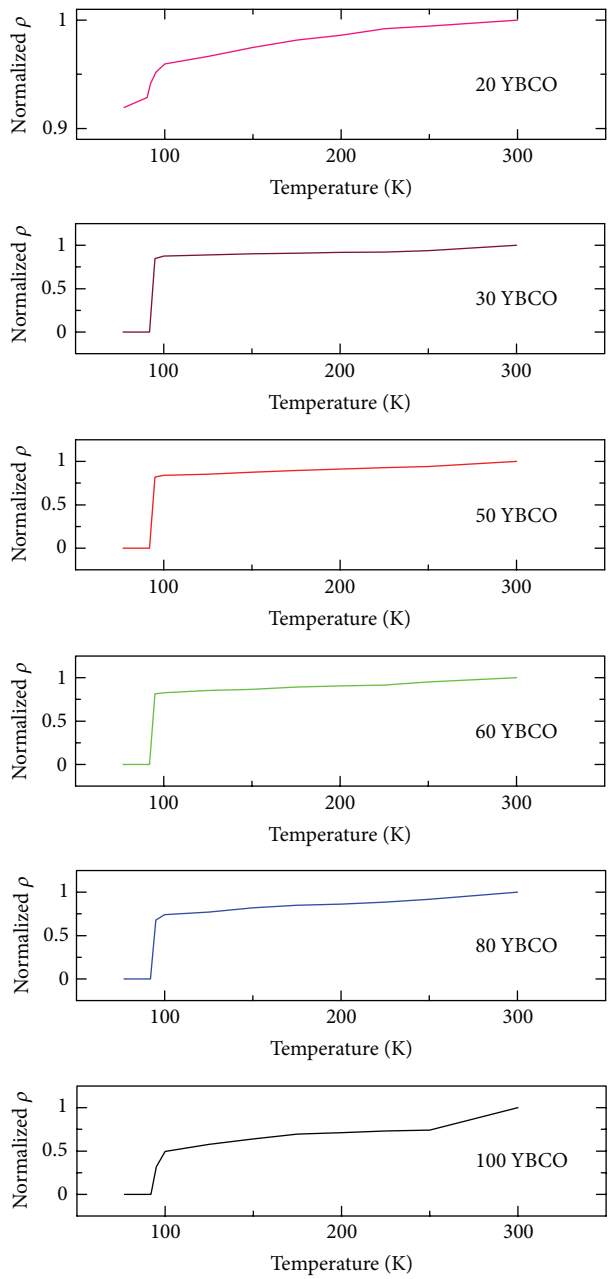

Figure 5: Temperature dependence of normalized with different volume percentages of SBNO.

of YBCO <30, the continuous network of superconducting grains breaks away and the resistance becomes nearly equal to that of pure insulator.

The variation of normal state resistivity for different vol% of SBNO in the composite are plotted in Figure 6.

The resistivity "ρ" and temperature coefficient of resistivity α at room temperature are also plotted as a function of vol.% of YBCO (V_S) in the composite. In the normal state, YBCO is a metallic conductor and shows resistivity ~1 mΩ cm. The normal state resistivity of YBCO-SBNO composite samples has shown a significant drop of ρ near $V_S \sim 26$ vol%.

The behavior of ρ correlates with that of α, which increases sharply towards that of YBCO starting from $V_S = 26$ vol%. Therefore, the percolation threshold value "V_C" for the normal state transport properties of the composite is ~26 vol% of YBCO. Thus, the superconducting percolation threshold and normal state percolation threshold values of YBCO-SBNO composites lie in the same range.

The normal state transport properties of ceramic insulator superconductor system can be described by a set of equation [23, 24]:

$$\begin{aligned} \rho &= \rho_o (V_S - V_C)^t \quad \text{for } V_S > V_C, \\ \rho' &= \rho_o' (V_C - V_S)^u \quad \text{for } V_C > V_S, \end{aligned} \tag{1}$$

where ρ and ρ' are constants and V_C is the critical volume fraction at which transport properties change drastically and

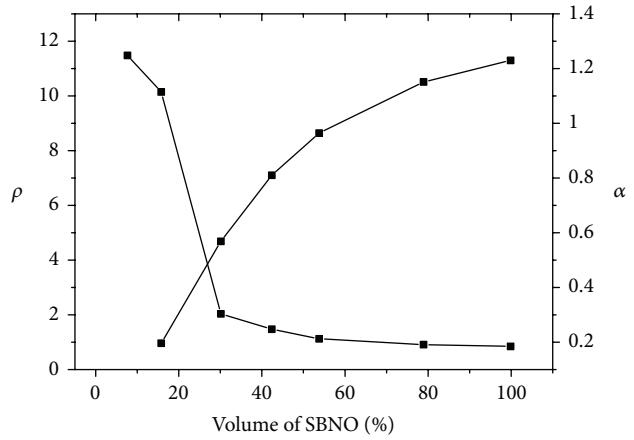

Figure 6: Variation of normal state resistivity and temperature coefficient of resistivity for different vol% of SBNO.

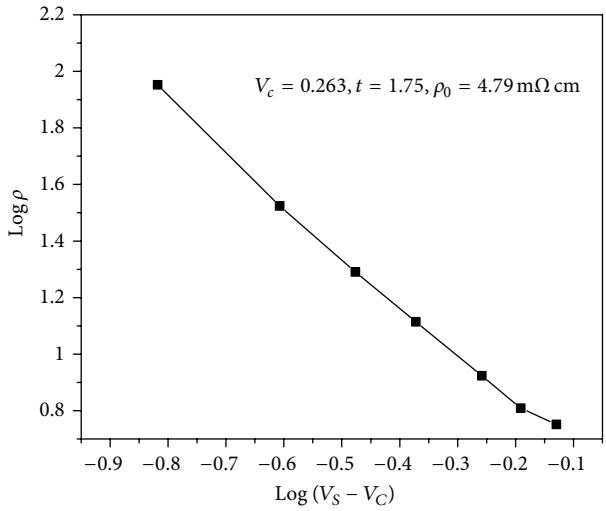

Figure 7: Log-log plot of ρ versus $(V_S - V_C)$.

it is called the percolation threshold. V_S is the vol.% of YBCO in the composite and "t" and "u" are the critical exponents describing the transport properties of the composite system.

The values of ρ_o, ρ_o', u, and t are found from a log-log plot of ρ versus $(V_S - V_C)$ and ρ' versus $(V_C - V_S)$. In the log-log plots of ρ versus $(V_S - V_C)$ shown in Figure 7 and ρ' versus $(V_C - V_S)$ given in Figure 8, respectively. Least-square fits were performed to determine the slope of the plots which gave the exponents "t" and "u" as 1.75 and 0.636, respectively, with a percolation threshold $V_C = 0.263$ and the values for ρ_0 and ρ_o' calculated as 4.79 mΩ cm and 12.76×10^{-11} mΩ cm, respectively. The values of critical exponents obtained for YBCO-SBNO composites agree reasonably well with the theoretical values for an idealized metal-insulator percolation system [25, 26].

The percolation studies carried out show that up to 75% addition of nano SBNO, YBCO preserved its superconducting property without any deterioration. The nonreactivity of YBCO with SBNO even at high processing temperature also

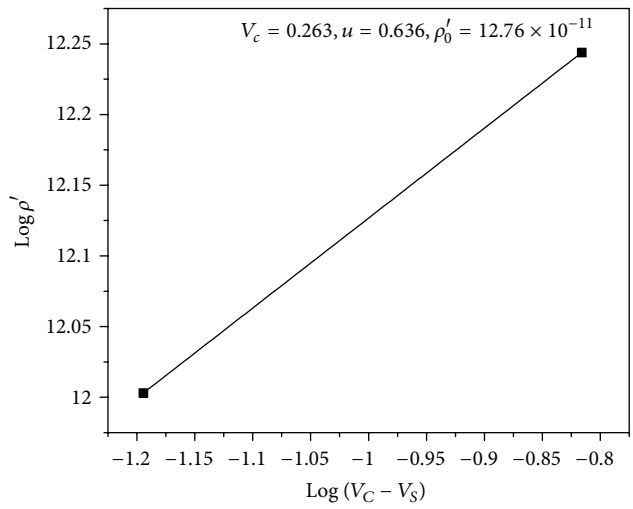

Figure 8: Log-log plot of ρ' versus $(V_C - V_S)$.

points to the fact that nano SBNO is a suitable substrate for YBCO super conductor.

4. Conclusion

Nanostructured $SmBa_2NbO_6$ ceramic powder synthesized by an auto igniting combustion technique was used for percolation study in YBCO-$SmBa_2NbO_6$ composite. The particle size calculated from the TEM image is the range 15–20 nm. The XRD study shows that the components of all compositions of the composites are nonreactive with each other even at high temperature. The samples are sintered in the temperature range 950–1350°C to its optimum density. SEM images showed that nanopowder was uniformly distributed within the bulk YBCO. YBCO preserved its superconductivity up to an addition of ~70% nano $SmBa_2NbO_6$. The obtained percolation threshold is ~26% for this superconductor-insulator composite. The critical exponents describing the transport properties of the composites are in good agreement with those of a perfect superconductor-insulator composite system. The chemical compatibility of $SmBa_2NbO_6$ with YBCO makes it a suitable nanoceramic substrate material for YBCO superconducting films.

Conflict of Interests

The authors declare that they have no conflict of interests.

Acknowledgments

The authors acknowledge the University Grants Commission (UGC) New Delhi, Council of Scientific and Industrial Research (CSIR) for the financial supports and Sophisticated Test and Instrumentation Centre (STIC), Cochin University of Science and Technology, Cochin, for experimental analysis.

References

[1] W. Gillijns, A. Y. Aladyshkin, A. V. Silhanek, and V. V. Moshchalkov, "Magnetic confinement of the superconducting condensate in superconductor-ferromagnet hybrid composites," *Physical Review B*, vol. 76, no. 6, Article ID 060503, 2007.

[2] M. I. Petrov, D. A. Balaev, D. M. Gohfeld, S. V. Ospishchev, K. A. Shaihudtinov, and K. S. Aleksandrov, "Applicability of the theory based on Andreev reflection to the description of experimental current-voltage characteristics of polycrystalline HTSC+normal metal composites," *Physica C*, vol. 314, no. 1, pp. 51–54, 1999.

[3] A. G. Mamalis, S. G. Ovchinnikov, M. I. Petrov et al., "Composite materials on high-T_c superconductors and $BaPbO_3$, Ag basis," *Physica C*, vol. 364-365, pp. 174–177, 2001.

[4] S. L. Huang, D. Dew-Hughes, D. N. Zheng, and R. Jenkins, "Effects of MgO addition on phase evolution and flux pinning of Bi-2212/Ag tapes fabricated by electrophoretic deposition and partial-melting processing," *Superconductor Science and Technology*, vol. 9, p. 368, 1996.

[5] K. Matsumoto, H. Takewaki, Y. Tanaka et al., "Enhanced Jc properties in superconducting NbTi composites by introducing Nb artificial pins with a layered structure," *Applied Physics Letters*, vol. 64, no. 1, pp. 115–117, 1994.

[6] N. McN Alfred, T. W. Button, and J. D. Birchall, "Processing, properties and devices in high-T_c superconductors," *Superconductor Science and Technology*, vol. 3, p. 1, 1990.

[7] A. Uarone and S. Pagano, in *Proceedings of the International Conference on Superconductivity (ICSC '90)*, S. K. Joshi, C. N. R. Rao, and S. V. Subramanyam, Eds., p. 310, World Scientific, Singapore, 1990.

[8] T. Van Duzer, "Superconductor electronics," *Cryogenics*, vol. 30, no. 12, pp. 980–995, 1990.

[9] G. Deutscher and K. A. Muller, "Origin of superconductive glassy state and extrinsic critical currents in high-T_c oxides," *Physical Review Letters*, vol. 59, article 1745, 1987.

[10] T. K. Worthington, W. J. Gallagher, and T. R. Dinger, "Anisotropic nature of high-temperature superconductivity in single-crystal $Y_1Ba_2Cu_3O_{7-x}$," *Physical Review Letters*, vol. 59, no. 10, pp. 1160–1163, 1987.

[11] M. P. A. Fisher, P. B. Weichman, G. Grinstein, and D. S. Fisher, "Boson localization and the superfluid-insulator transition," *Physical Review B*, vol. 40, no. 1, pp. 546–570, 1989.

[12] M. P. A. Fisher, "Quantum phase transitions in disordered two-dimensional superconductors," *Physical Review Letters*, vol. 65, pp. 923–926, 1990.

[13] S. L. Sondhi, S. M. Girvin, J. P. Carini, and D. Shahar, "Continuous quantum phase transitions," *Reviews of Modern Physics*, vol. 69, no. 1, pp. 315–333, 1997.

[14] A. Finkelshtein, "Suppression of superconductivity in homogeneously disordered systems," *Physica B*, vol. 197, pp. 636–648, 1994.

[15] S. Maekawa and H. Fukuyama, "Localization effects in two-dimensional superconductors," *Journal of the Physical Society of Japan*, vol. 51, no. 5, pp. 1380–1385, 1982.

[16] D. Belitz, "Relation between the T_c degradation and the correlation gap in disordered superconductors," *Phys. Rev. B*, vol. 40, pp. 111–114, 1989.

[17] K. V. Mitsen and O. M. Ivanenko, "Local structure, percolation and insulator-conductor transition in doped HTS," *Physica C*, vol. 341-348, no. 2, pp. 1849–1850, 2000.

[18] N. Marković, C. Christiansen, A. M. Mack, W. H. Huber, and A. M. Goldman, "Superconductor-insulator transition in two dimensions," *Physical Review B*, vol. 60, no. 6, pp. 4320–4328, 1999.

[19] Y. M. Strelniker, A. Frydman, and S. Havlin, "Percolation model for the superconductor-insulator transition in granular films," *Physical Review B*, vol. 76, no. 22, Article ID 224528, 2007.

[20] J. Koshy, J. K. Thomas, J. Kurian, Y. P. Yadava, and A. D. Damodaran, "Superconducting $YBa_2Cu_3O_{7-\delta}$ thick film ($T_{c(0)}$ = 92 K) on $SmBa_2NbO_6$: a newly developed perovskite ceramic substrate," *Physica C*, vol. 215, no. 1-2, pp. 209–212, 1993.

[21] J. K. Thomas, J. Koshy, J. Kurian, Y. P. Yadava, and A. D. Damodaran, "Electrical transport and superconductivity in $YBa_2Cu_3O_{7-\delta}$ -$YBa_2HfO_{5.5}$ percolation system," *Journal of Applied Physics*, vol. 76, no. 4, p. 2376, 1994.

[22] K. V. Paulose, J. Koshy, and A. D. Damodaran, "YBa_2NbO_6: synthesis, properties and compatibility with $YBa_2Cu_3O_{7-\delta}$," *Physica C*, vol. 193, no. 3-4, pp. 273–276, 1992.

[23] D. Stauffer, "Scaling theory of percolation clusters," *Physics Reports*, vol. 54, pp. 1–74, 1979.

[24] J. P. Straley, "Scaling predictions for physical properties," in *Percolation Structures and Processes*, G. Deutscher, R. Zallen, and J. Adler, Eds., p. 353, Israel Physical Society, 1983.

[25] J. J. Lin, W. Y. Lin, and R. F. Tsui, "Electrical transport and superconductivity in the Al_2O_3-$Bi_2Sr_{1.8}Ca_{1.2}Cu_2Oy$ and MgO-$Bi_2Sr_{1.8}Ca_{1.2}Cu_2Oy$ composites," *Physica C*, vol. 210, pp. 455–462, 1993.

[26] J. Kerteszi and T. Vicsek, in *Sinteritzg Theory and Practice*, D. Kolar, S. Iejovnik, and M. M. Ristic, Eds., p. 53, Elsevier Scientific, Amsterdam, The Netherlands, 1982.